Effects of Multiple Pathways on Excited-State Energy Flow in Self-Assembled Wheel-and-Spoke Light-Harvesting Architectures

Hee-eun Song,[†] Christine Kirmaier,[†] Jennifer K. Schwartz,[†] Eve Hindin,[†] Lianhe Yu,[‡] David F. Bocian,[§] Jonathan S. Lindsey,[‡] and Dewey Holten*,[†]

Department of Chemistry, Washington University, St. Louis, Missouri 63130-4889, Department of Chemistry, North Carolina State University, Raleigh, North Carolina 27695-8204, and Department of Chemistry, University of California at Riverside, Riverside, California 92521-0403

Received: June 26, 2006; In Final Form: July 25, 2006

Static and time-resolved optical measurements are reported for three cyclic hexameric porphyrin arrays and their self-assembled complexes with guest chromophores. The hexameric hosts contain zinc porphyrins and 0, 1, or 2 free base (Fb) porphyrins (denoted Zn_6, Zn_5Fb, or Zn_4Fb_2, respectively). The guest is a core-modified (O replacing one of the four N atoms) dipyridyl-substituted Fb porphyrin (DPFbO) that coordinates to zinc porphyrins of a host via pyridyl−zinc dative bonding. Each architecture is designed to have a gradient of excited-state energies for excitation funneling among the weakly coupled constituents of the host to the guest. Energy transfer to the lowest-energy chromophore(s) (coordinated zinc porphyrins or Fb porphyrins) within a hexameric host occurs primarily via a through-bond (TB) mechanism, is rapid (∼40 ps), and is essentially quantitative (≥98%). Energy transfer from a pyridyl-coordinated zinc porphyrin of the host to the guest in the Zn_6·DPFbO complex has a yield of ∼75%, a rate constant of $\sim(0.7\ ns)^{-1}$, and significant Förster through-space (TS) character. In the case of Zn_5Fb·DPFbO, which has an additional TS route via the Fb porphyrin with a rate constant of $\sim(20\ ns)^{-1}$, the yield of energy transfer to the guest is somewhat lower (∼50%) than that for Zn_6·DPFbO. Complex Zn_4Fb_2·DPFbO has an identical TS pathway via the Fb porphyrin plus an additional TS pathway involving the second Fb porphyrin (closer to the guest) with a rate constant of $\sim(0.5\ ns)^{-1}$. This complex exhibits an energy-transfer yield to the guest that is significantly enhanced over that for Zn_5Fb·DPFbO and comparable to that for Zn_6·DPFbO. Collectively, the results for the various arrays suggest designs for similar host−guest complexes that are expected to exhibit much more efficient light harvesting and excitation trapping at the central guest chromophore.

I. Introduction

In the companion paper we characterized the energy flow in a self-assembled host−guest complex.[1] The host molecule consisted of a cyclic array of six zinc porphyrins joined via diarylethyne linkers (Zn_6). The guest molecule consisted of a tripyridyl arene, or more interestingly, a dipyridyl-substituted free base (Fb) porphyrin (DPFb) that coordinates to zinc porphyrins of a host via pyridyl−zinc dative bonding. Upon absorption of light by a porphyrin in the host of the host−guest complex (Zn_6·DPFb), excited-state energy rapidly migrated to the pyridyl-coordinated zinc porphyrins (Zn_C) via a through-bond (TB) mechanism. A slower, through-space (TS) energy-transfer process ensued from the Zn_C to the DPFb guest. The overall energy-transfer efficiency to the guest Fb porphyrin is 65%. This includes transfer among the zinc porphyrins in the backbone of the cyclic array.

The sluggishness of energy transfer from the Zn_C to the guest porphyrin prompted the design of arrays wherein additional pathways of transfer might afford increased overall efficiency. In the Zn_6·DPFb host−guest complex, the Zn_C porphyrins have a lifetime in the absence of energy transfer of ∼2 ns. A strategy to enhance the yield of energy flow to the guest is to use a donor within the hexamer that has a much longer excited-state lifetime. The obvious choice is a Fb porphyrin ($\tau \approx 13$ ns), for which energy transfer to the guest necessarily would be TS in character. Two cyclic hexameric arrays that enable this design are shown in Chart 1. The arrays are comprised of one or two Fb porphyrins and are denoted Zn_5Fb or Zn_4Fb_2, respectively. (Note that the Zn_3Fb_3 array examined in the companion paper is not suitable because the zinc porphyrins in the host are not properly located for guest binding to the interior of the array.) The use of a Fb porphyrin as a donor also requires a longer-wavelength absorbing guest, for which we chose the Fb oxaporphyrin DPFbO (Chart 1). The DPFbO porphyrin has one core nitrogen replaced with oxygen and bears two pyridyl groups (analogous to DPFb) to enable coordination to the host via pyridyl−zinc dative bonding. The resulting self-assembled host−guest complexes are Zn_5Fb·DPFbO and Zn_4Fb_2·DPFbO (Chart 2).

In this paper, we report the dynamics of excited-state energy flow in the two cyclic hexameric arrays, Zn_5Fb and Zn_4Fb_2, as well as three self-assembled host−guest complexes, Zn_6·DPFbO, Zn_5Fb·DPFbO, and Zn_4Fb_2·DPFbO. The latter two architectures have one or two Fb porphyrins, respectively, that can serve as long-lived excited-state way stations for energy flow to the guest chromophore. The studies yield the unexpected result that host−guest energy transfer in Zn_4Fb_2·DPFbO and Zn_5Fb·DPFbO is

* Author to whom correspondence should be addressed. E-mail: holten@wustl.edu.
[†] Washington University.
[‡] North Carolina State University.
[§] University of California at Riverside.

10.1021/jp064001a CCC: $33.50
Published on Web 09/13/2006

CHART 1

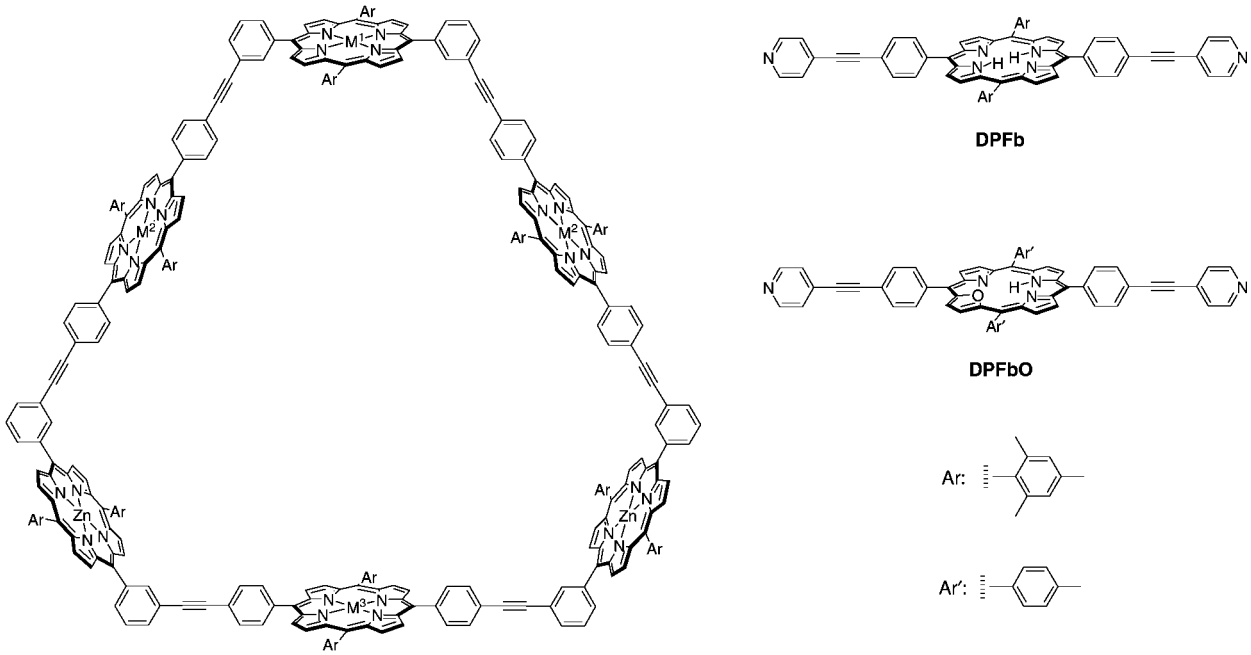

actually somewhat less efficient than that in Zn_6·DPFbO. Together, the results elucidate designs for cyclic hexameric arrays containing different placements of zinc and Fb porphyrins that are expected to exhibit much more efficient excitation trapping at the central guest chromophore. An added challenge is to combine these insights with recent advances in the synthesis of multiporphyrin architectures[2−24] to build more efficient light-harvesting complexes.

II. Experimental Methods

The cyclic hexamer hosts (Zn_6,[25] Zn_5Fb,[26] and Zn_4Fb_2[26]), guest (DPFbO[26]), and reference monomers (ZnU, FbU)[27] were prepared as described previously. The self-assembled host−guest complexes (Zn_6·DPFbO, Zn_5Fb·DPFbO, and Zn_4Fb_2·DPFbO) were prepared via titrations of stock toluene solutions of the host and guest compounds as described previously[25,28] and in the Supporting Information. All of the above arrays were studied in toluene. The arrays Zn_6·pyr_6, Zn_3Fb_3·pyr_3, and ZnU·pyr, in which each of the zinc porphyrins is singly coordinated by a pyridine (pyr) ligand, were prepared as described previously.[1] Static and time-resolved optical studies and kinetic modeling were conducted as described in the companion paper.[1]

III. Results and Discussion

A. Energy-Transfer Pathways and Mechanisms. Chart 3 gives schematic representations of the hexameric arrays and host−guest complexes, along with associated kinetic pathways. For clarity, only one process of a given type is indicated within each array even though the process may occur multiple times due to symmetry. As discussed in the companion paper,[1] we assume on the basis of prior results that the energy-transfer dynamics are the same whether the donor and acceptor are attached to the *m*- and *p*-positions, respectively, of the phenyl rings of the diphenylethyne linker (denoted *m*/*p* connectivity) or vice versa (denoted *p*/*m* connectivity). Also, a zinc porphyrin that is axially coordinated (Zn_C) has its first excited singlet state at lower energy than an uncoordinated zinc porphyrin (Zn_U). On the basis of the average (0,0) absorption and fluorescence wavelengths, the excited-state energy decreases in the order: Zn_U (2.08 eV) > Zn_C (2.04 eV) > DPFb (1.91 eV) > DPFbO (1.83 eV). This energy ordering is a key determinant of the directions and pathways of energy flow in the arrays.

The dynamics of energy flow in the cyclic hexameric arrays Zn_5Fb and Zn_4Fb_2 are expected to embody the same types of processes observed in diverse acyclic arrays composed of zinc and Fb porphyrins. A number of the rate constants that underlie the dynamics of energy flow in the arrays are available from studies described in the companion paper (Table 1). The present paper elucidates the rates associated with transfer to the guest oxaporphyrin DPFbO and additional processes that stem from the presence of additional pathways for energy flow in Zn_5Fb, Zn_4Fb_2, and their host−guest complexes. In Zn_6·DPFbO, the final trapping step is expected to be Zn_C^*DPFbO → Zn_C DPFbO* (M_4; Chart 3B), analogous to that occurring in Zn_6·DPFb (M_1; Chart 3A).[1] In the host−guest arrays Zn_4Fb_2·DPFbO and Zn_5Fb·DPFbO (Charts 3C and 3D), energy could flow to the DPFbO guest chromophore via the Zn_C (M_4) or via the Fb porphyrins (M_7 and M_8). Array Zn_5Fb·DPFbO has one Fb*DPFbO→ FbDPFbO* route available while Zn_4Fb_2·DPFbO has two, and the latter are expected to differ in rate due to the distances involved (Chart 2A; 20.9 versus 14.2 Å). To facilitate the presentation of the results, Table 2 summarizes the time constants of the kinetic components derived from the transient-absorption measurements. The table also contains the associated fluorescence yields and lifetimes, which are dominated by the lowest-energy site(s) in each architecture.

B. Energy Transfer in the Hexameric Hosts. Transient-absorption difference spectra for Zn_4Fb_2 and Zn_5Fb are shown in Figures 1A and 1B, and associated kinetic data are shown in

CHART 2

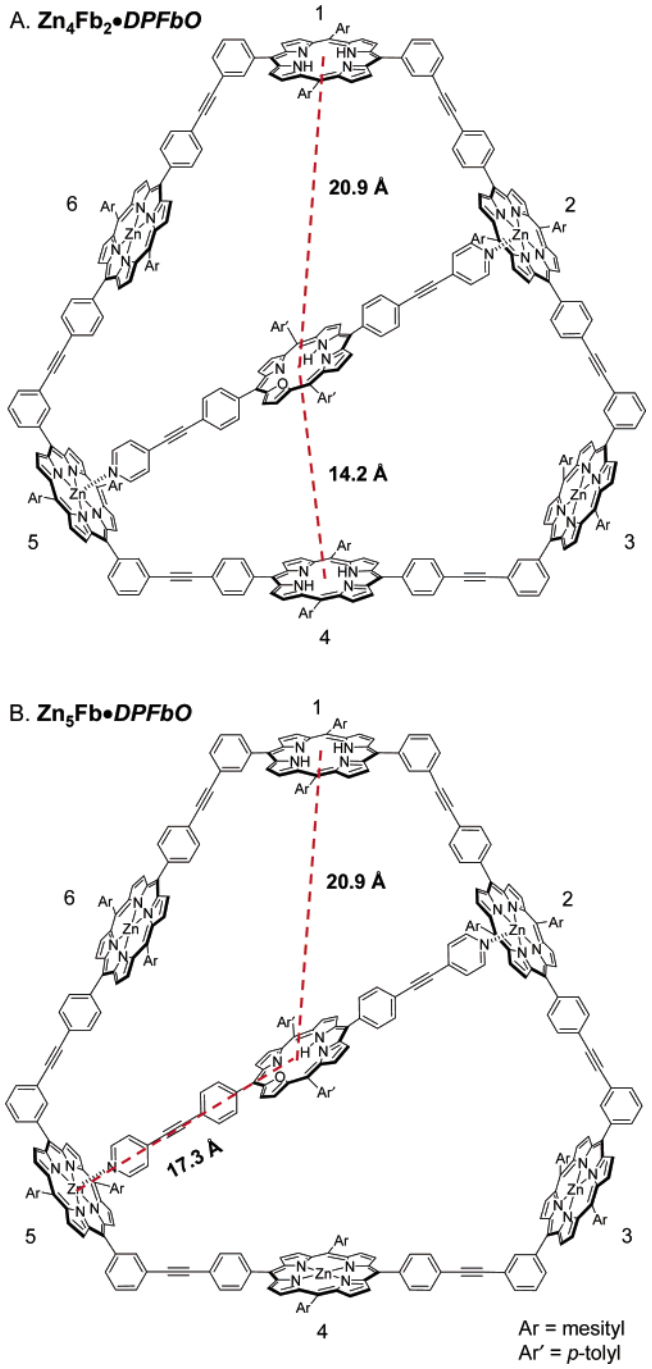

Figure 2. The transient spectra are dominated by features comprised of bleaching of the ground-state absorption bands and excited-state stimulated emission (fluorescence stimulated by the white-light probe pulse). The positions of the features are approximated by those in the static absorption and fluorescence spectra of the species involved (Figure 1C). On the basis of these comparisons, the spectra at 1 ps for Zn_4Fb_2 and Zn_5Fb are assigned primarily to Zn_U^* produced by the excitation flash. Similarly, the spectrum at the longest time for each array is assigned to Fb*, which has a fluorescence lifetime (~13 ns) typical of those for monomeric reference compounds (Table 2).

The time evolution of the transient difference spectra for both Zn_4Fb_2 and Zn_5Fb shows a minor fast (~3 ps) component that is not present for arrays such as hexamer Zn_3Fb_3 or the dyad ZnFb-*m*/*p*.[1,25] However, such a transient is observed for ZnZn-*m*/*p* (2.7 ± 0.3 ps) and ZnZn·pyr$_2$ (3.6 ± 0.8 ps)[1] and other arrays containing adjacent zinc porphyrins.[29,30] This minor fast component is assigned to $Zn_U^*Zn_U^* \rightarrow Zn_U^*Zn_U$ excited-state annihilation in a small fraction of the arrays in which two zinc porphyrins are both excited.

The overall kinetics for $Zn_U^*Fb \rightarrow Zn_UFb^*$ energy flow for Zn_4Fb_2 occurs with a time constant of 36 ± 4 ps. For Zn_5Fb, a much longer average time constant of 150 ± 50 ps is observed (along with a minor ~25 ps phase that improves the fits at some wavelengths). The pronounced lengthening of the time course of energy flow for Zn_5Fb compared to Zn_4Fb_2 can be seen from visual inspection of the kinetic data in Figure 2. Whereas ΔA for Zn_4Fb_2 has reached a constant value (due to Fb*) by 200 ps, the signal for Zn_5Fb continues to decay well past this point.

The source of the significant lengthening of energy flow in Zn_5Fb (150 ps) compared to Zn_4Fb_2 (36 ps) is explained by the molecular architectures of the two arrays and how these structures determine the number of steps necessary for excitation on the most distant zinc porphyrin to reach a Fb unit (Charts 3G and 3H). In Zn_4Fb_2, each zinc porphyrin is adjacent to a Fb trap. This is not the case for Zn_5Fb, for which each first nonnearest neighbor is separated from the trap by a zinc porphyrin affording a bidirectional $Zn_U^*Zn_U \rightleftarrows Zn_UZn_U^*$ energy-transfer step (k_2). In addition, the zinc porphyrin that is trans to the Fb porphyrin (its second nonnearest neighbor) is separated by two zinc porphyrins, affording two such reversible energy-transfer steps. Furthermore, two superexchange-mediated nonadjacent energy-transfer processes are operable: a bidirectional transfer between zinc porphyrins (L_2) and a unidirectional transfer to the trap from a zinc porphyrin (L_4). The consequence is that excitation of any of the zinc porphyrins in Zn_5Fb that are nonadjacent to the Fb porphyrin, either by direct photon absorption or energy transfer, will lead to a lengthening of the effective Zn_U^* decay and the arrival time of the excitation on the Fb porphyrin.

The kinetic modeling reproduces the dominant kinetic phase of 36 ± 4 ps for Zn_4Fb_2 and 150 ± 50 ps for Zn_5Fb, using the value of $k_1 = (38\ \text{ps})^{-1}$ for $Zn_U^*Fb \rightarrow Zn_UFb^*$ determined from Zn_3Fb_3.[1,25] The kinetics for Zn_4Fb_2 give $L_4 \leq (300\ \text{ps})^{-1}$. The expected value of k_2 for bidirectional $Zn_U^*Zn_U \rightleftarrows Zn_UZn_U^*$ energy transfer in Zn_4Fb_2 is ~$(50\ \text{ps})^{-1}$ based on the arguments given in the companion paper;[1] however, the overall rate derived from the kinetic modeling is not particularly sensitive to the rate constant for this process over the range from $(20\ \text{ps})^{-1}$ to $(100\ \text{ps})^{-1}$ because each zinc porphyrin is adjacent to a trap (Chart 3G). For Zn_5Fb, the dynamics are reproduced using $k_1 = (38\ \text{ps})^{-1}$, $k_2 = (50-100\ \text{ps})^{-1}$, $L_4 \leq (300\ \text{ps})^{-1}$, and $L_2 = (1-3\ \text{ns})^{-1}$ (Chart 3H). These rate constants are listed in Table 1. The modeling also associates the minor ~25 ps component observed at some wavelengths for Zn_5Fb with the time evolution of the zinc porphyrins immediately adjacent to the trap; the population dynamics indicate that this component will be difficult to resolve if the associated spectral features significantly overlap (as they do). The modeled excited-state populations give a yield of 0.99 for energy transfer to the Fb porphyrin(s) in Zn_4Fb_2 and Zn_5Fb, independent of coordination state of the zinc porphyrin light-harvesting elements. These high yields are consistent with the transient-absorption kinetics, fluorescence spectra, and fluorescence yields.

Collectively, the above findings on the rates and yields of energy transfer to the lowest-energy component(s) in the hexameric wheels are essential for understanding the dynamics in the host−guest complexes described next. These values will be used in the analysis of energy flow in the latter arrays, which

CHART 3

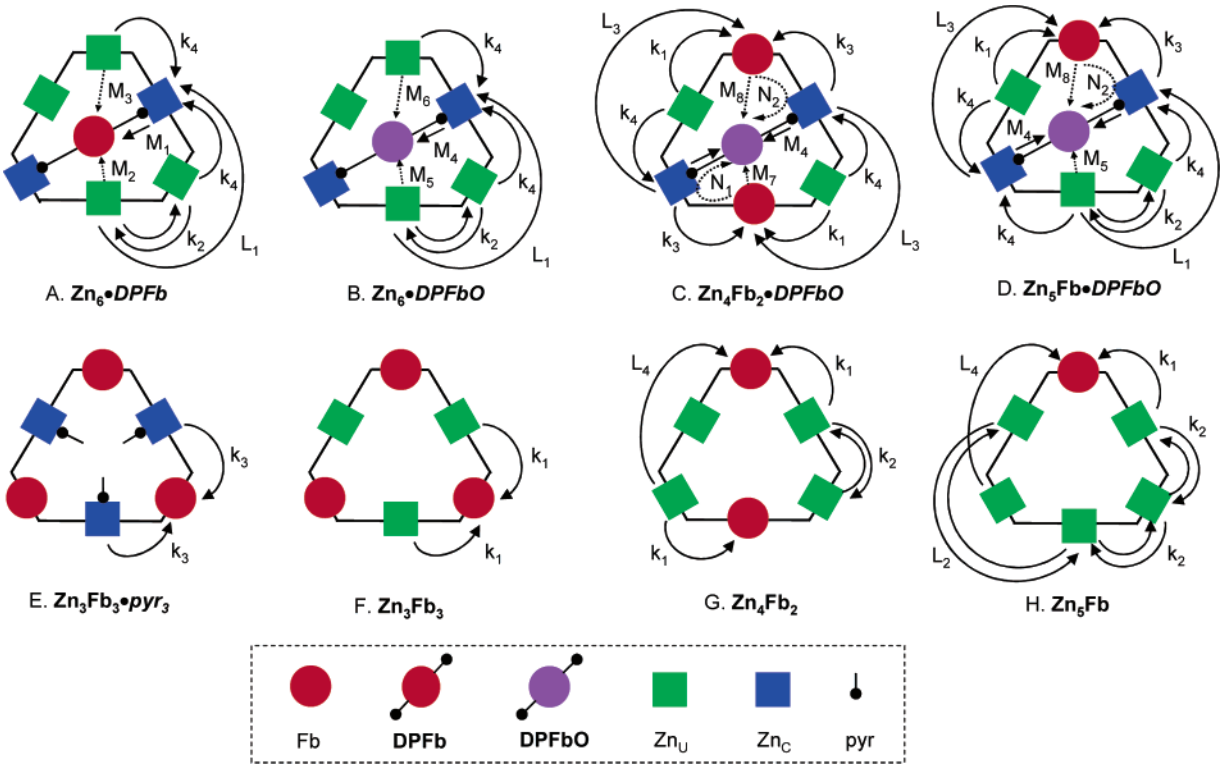

TABLE 1: Summary of Rate Constants[a]

rate constant	(value)$^{-1}$
From Companion Paper[b]	
k_1	38 ps
k_3	38 ps
k_4	42 ps
M_1	1.1 ns
	0.82 ns[c]
M_2	0.26 ns[c]
M_3	2.6 ns[c]
L_1	≥0.2 ns
Determined Here	
k_2	20−100 ps[d]
M_4	0.73 ns
	0.97 ns[c]
M_5	0.45 ns[c]
M_6	4.5 ns[c]
$M_7 + N_1$	0.53 ns
$M_8 + N_2$	20 ns
L_2	1−3 ns
L_3	1.5 ns
L_4	≥0.3 ns

[a] See Chart 3 for definition of rate constants. The values were derived from the measured and modeled transient-absorption kinetics unless indicated otherwise. [b] From ref 1. [c] From Förster calculations in Table 3. [d] The expected value of $(k_2)^{-1}$ is ∼50 ps,[1] but only a range could be derived from kinetic modeling for Zn_4Fb_2 and Zn_5Fb.

TABLE 2: Summary of Photophysical Data[a]

	transient-absorption lifetime components (ps)			fluorescence			
					τ (ns)[b]		
compounds	*c*	*d*	*e*	Φ_f	Zn	Fb_{host}	Fb_{guest}
Host−Guest Complexes							
Zn_6•DPFb[f]	3.1 ± 0.7	33 ± 9	730 ± 80	0.084	0.9		11
Zn_6•DPFbO	2.7 ± 0.3	40 ± 10	540 ± 70	0.057	1.0		10
Zn_4Fb_2•DPFbO		30 ± 10	510 ± 30	0.083		1.7[g]	11
Zn_5Fb•DPFbO	3 ± 1	30 ± 10	400 ± 100	0.065		8	12
Hexameric Hosts							
Zn_6				0.040	2.4		
Zn_5Fb	3 ± 1	25 ± 5	150 ± 50	0.084		13	
Zn_4Fb_2	3 ± 1	36 ± 4		0.10		13	
Guest							
DPFbO				0.12			11

[a] All data were obtained in toluene at room temperature. [b] Lifetimes ±7%. [c] Excited-state annihilation. [d] Energy transfer within the hexameric host. [e] Time constant of one phase of energy flow, most often the lifetime of the shortest-lived energy donor to the guest. [f] From ref 1. [g] Also fit well by two components with lifetimes of 8 ns (fixed) and 0.8 ± 0.3 ns.

exhibit the same processes within the host plus one or more additional pathways for energy trapping by the guest chromophore.

C. Energy Transfer in the Host−Guest Complexes. *1. Zn_6•DPFbO.* Figure 3 compares the absorption and fluorescence spectra of Zn_6, DPFbO, and the Zn_6•DPFbO complex. These spectra show that fluorescence from Zn_6•DPFbO derives primarily from the guest porphyrin, even when a zinc porphyrin of the host is principally excited at 550 nm. Likewise, the time-resolved fluorescence of the host−guest complex has a dominant component (10 ± 1 ns) that is comparable to that for an isolated DPFbO. A shorter (∼1 ns) component is assigned to the Zn_C porphyrins (Chart 3B), whose lifetime is better determined from the transient-absorption data described below. The static fluorescence data give a yield of 0.40 for Zn_C^*DPFbO → Zn_CDPFbO* energy transfer in Zn_6•DPFbO.

Further details on the energy flow in Zn_6•DPFbO are derived from transient-absorption studies (Figure 4A). The time evolution of the features analyzed using the reference spectra in Figure 4B are readily attributed to net energy flow from Zn_U to Zn_C porphyrins within the hexamer, followed by energy transfer to the DPFbO guest. Kinetic traces (Supporting Information) give time constants of ∼3 ps, 40 ± 10 ps, and 540 ± 70 ps. The kinetic components are assigned in analogy to those for Zn_6•DPFb in the companion paper.[1] In particular, the minor ∼3 ps phase is assigned to excited-state annihilation in a small fraction

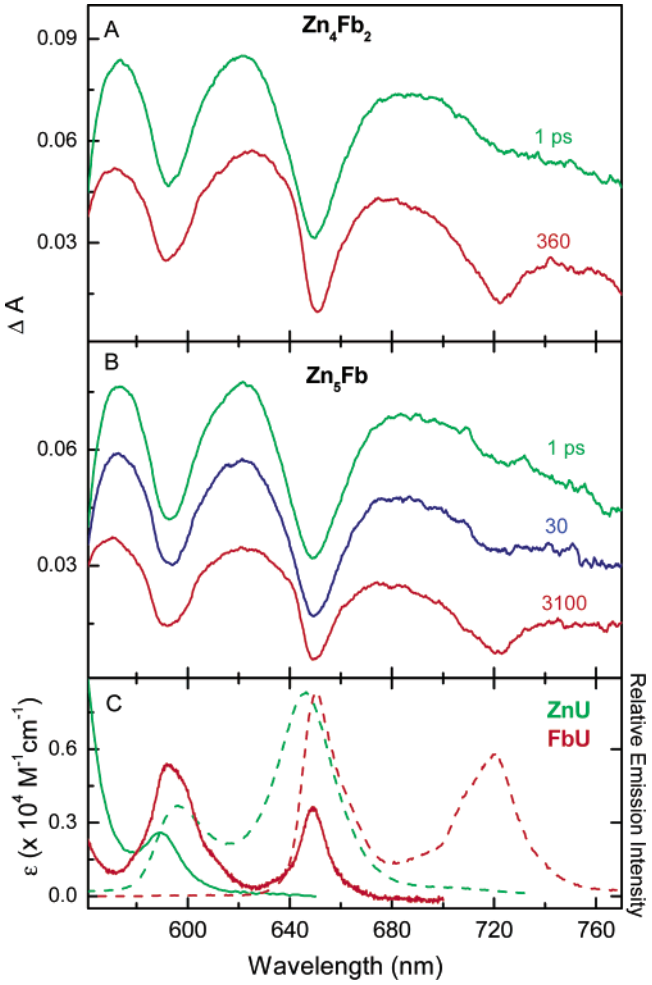

Figure 1. Transient-absorption spectra obtained using a 130 fs excitation flash at 540 nm for (A) Zn_4Fb_2 and (B) Zn_5Fb. Panel C shows absorption (solid lines) and fluorescence (dashed lines) spectra of reference compounds ZnU (green) and FbU (red).

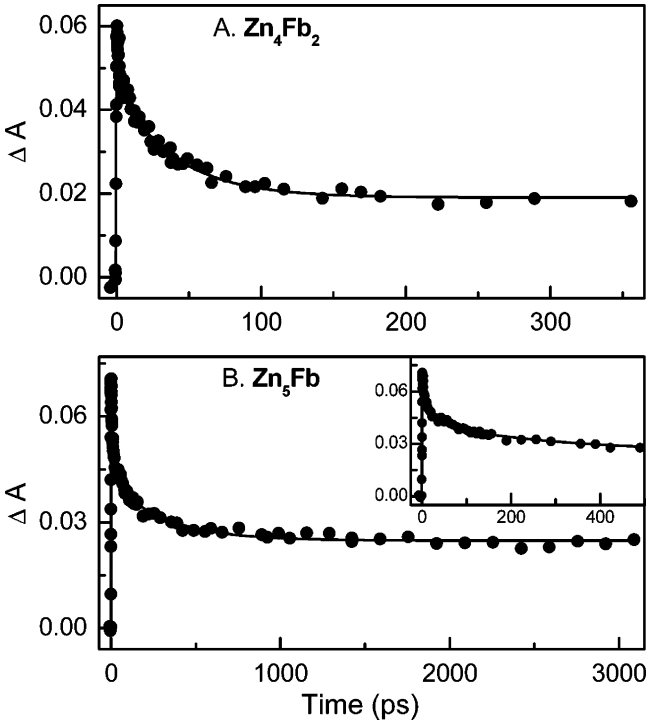

Figure 2. Kinetic data for Zn_4Fb_2 and Zn_5Fb measured at 730 and 685 nm, respectively, following excitation with a 130 fs flash at 540 nm. The fits use (A) dual or (B) triple exponentials plus a constant along with the instrument response. The time constants are discussed in the text.

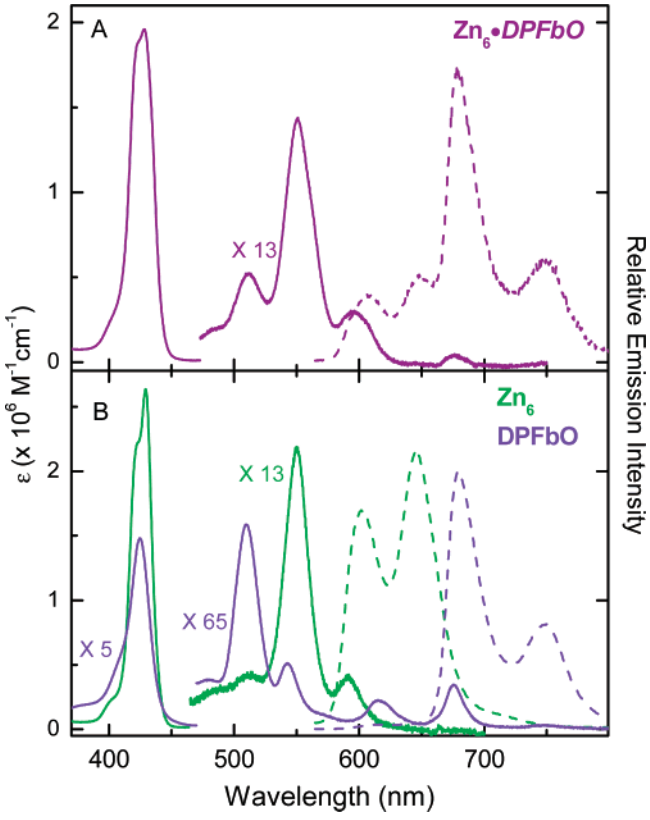

Figure 3. Absorption (solid lines) and fluorescence (dashed lines) spectra of (A) Zn_6•DPFbO (purple) and (B) Zn_6 (green) and DPFbO (violet).

of the arrays, the ~40 ps component to energy flow among the zinc porphyrins of the host to form an excited bookend zinc porphyrin Zn_C^*, and the 540 ps component to the Zn_C^* lifetime. The latter value is much shorter than the Zn_C^* lifetime of 2.1 ns for Zn_6•pyr_6. Thus, the transient-absorption data give a yield for host-to-guest energy transfer of $\Phi_{trans} = 1 - (0.54/2.1) = 0.74$. This value is somewhat larger than that obtained from the fluorescence spectra. Considering the relative errors in these measurements, we report $\Phi_{trans} = 0.74$ for the Zn_C^*DPFbO → Zn_CDPFbO* energy-transfer process in Zn_6•DPFbO (Chart 3B). The corresponding rate constant is $M_4 = [(0.54)^{-1} - (2.1\ ns)^{-1}] = (0.73\ ns)^{-1}$.

The above-measured values are comparable to the calculated Förster efficiency $\Phi_{TS} = 0.69$ and rate $k_{TS} = (0.97\ ns)^{-1}$ (Table 3). These measured and calculated values for Zn_6•DPFbO are comparable to the measured $\Phi_{trans} = 0.65$ and $M_1 = (1.1\ ns)^{-1}$ and calculated Förster rate $k_{TS} = (0.82\ ns)^{-1}$ for Zn_C^*DPFb → Zn_CDPFb* in the analogous Zn_6•DPFb complex studied in the companion paper.[1] Thus, TS energy transfer makes a major contribution to the final stage of energy flow in both host−guest architectures. Furthermore, Förster calculations and kinetic modeling indicate that the rates of TS energy transfer from Zn_U^* to the guest in Zn_6•DPFbO (M_5 and M_6) are noncompetitive with energy transfer to the Zn_C bookend units, as was found[1] for the analogous processes (M_2 and M_3) for Zn_6•DPFb (Charts 3A and 3B and Table 3). Thus, the yields of energy transfer from Zn_C^* to the guest porphyrin in both arrays are also effectively the yields for overall host → guest energy trapping.

2. Zn_4Fb_2•DPFbO and Zn_5Fb•DPFbO. Fluorescence from

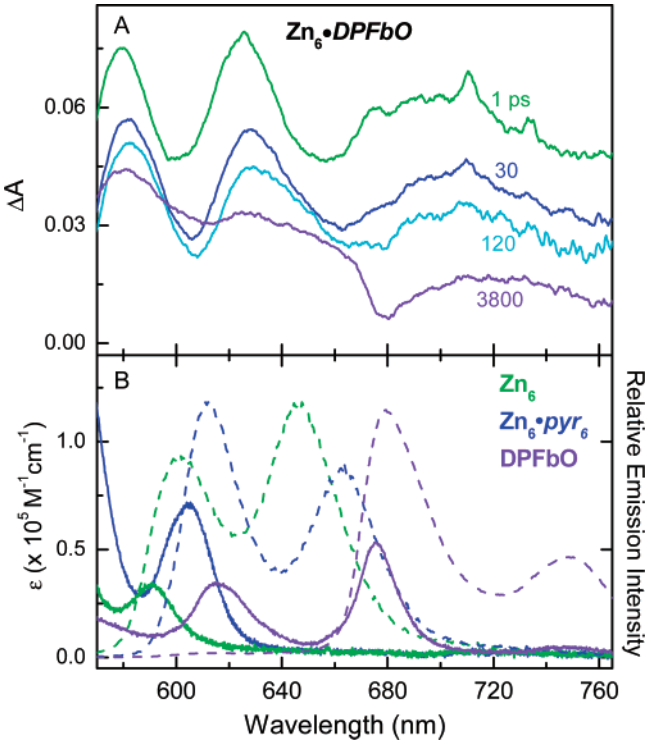

Figure 4. Transient-absorption spectra obtained using a 130 fs excitation flash at 540 nm for (A) Zn_6·DPFbO. Panel B shows absorption (solid lines) and fluorescence (dashed lines) spectra of Zn_6 (green), Zn_6·pyr_6 (blue), and DPFbO (violet). Note that the amplitude of the spectrum of DPFbO has been magnified 10-fold.

TABLE 3: Förster Energy-Transfer Parameters[a]

donor	acceptor	rate constant	R (Å)	quantum yield	donor lifetime (ns)	$J \times 10^{14}$ (cm^6)	Φ_{TS}	$(k_{TS})^{-1}$ (ns)
Zn_C	DPFb	M_1	17.3	0.037	2.2	4.43	0.73	0.82
Zn_U	DPFb	M_2	14.2	0.034	2.4	5.17	0.90	0.26
Zn_U	DPFb	M_3	20.9	0.034	2.4	5.17	0.48	2.6
Zn_C	DPFbO	M_4	17.3	0.037	2.2	3.75	0.69	0.97
Zn_U	DPFbO	M_5	14.2	0.034	2.4	2.97	0.84	0.45
Zn_U	DPFbO	M_6	20.9	0.034	2.4	2.97	0.35	4.5
FbU	DPFbO	M_7	14.2	0.12	13	2.12	0.93	0.96
FbU	DPFbO	M_8	20.9	0.12	13	2.12	0.57	9.7

[a] Calculations used PhotochemCAD[32] with $\kappa^2 = 0.25$. Distances were obtained as described in ref 25. Donor lifetimes and quantum yields are taken from ref 1. For donor Zn_C and Zn_U, the fluorescence parameters for ZnU·pyr and ZnU, respectively, were utilized. For acceptor DPFbO, an extinction coefficient $\log(\epsilon) = 5.47$ at 425 nm was used from ref 26. The calculations for complexes using the DPFb acceptor were performed in ref 1.

both Zn_5Fb·DPFbO and Zn_4Fb_2·DPFbO has a substantial contribution from the DPFbO guest, along with contributions from the zinc and Fb porphyrins in the host (Supporting Information). These data show that energy can effectively reach the guest from the host in each array. However, due to overlapping spectral contributions, the energy-transfer yields and rates are best determined from time-resolved studies.

The results of time- and wavelength-resolved fluorescence studies contribute to the analysis. Probing at 680 nm, where DPFbO should primarily emit, gives lifetimes of 12 ± 1 ns for Zn_5Fb·DPFbO and 11 ± 1 ns for Zn_4Fb_2·DPFbO. These values are comparable to the 11 ± 1 ns lifetime for isolated DPFbO. At 650 nm, fluorescence from the guest is minimal while that from the Fb porphyrins in the host is maximal. The fluorescence-decay profile at 650 nm for Zn_5Fb·DPFbO is fit well with a time constant of 8 ± 1 ns, which we assign to the lifetime of

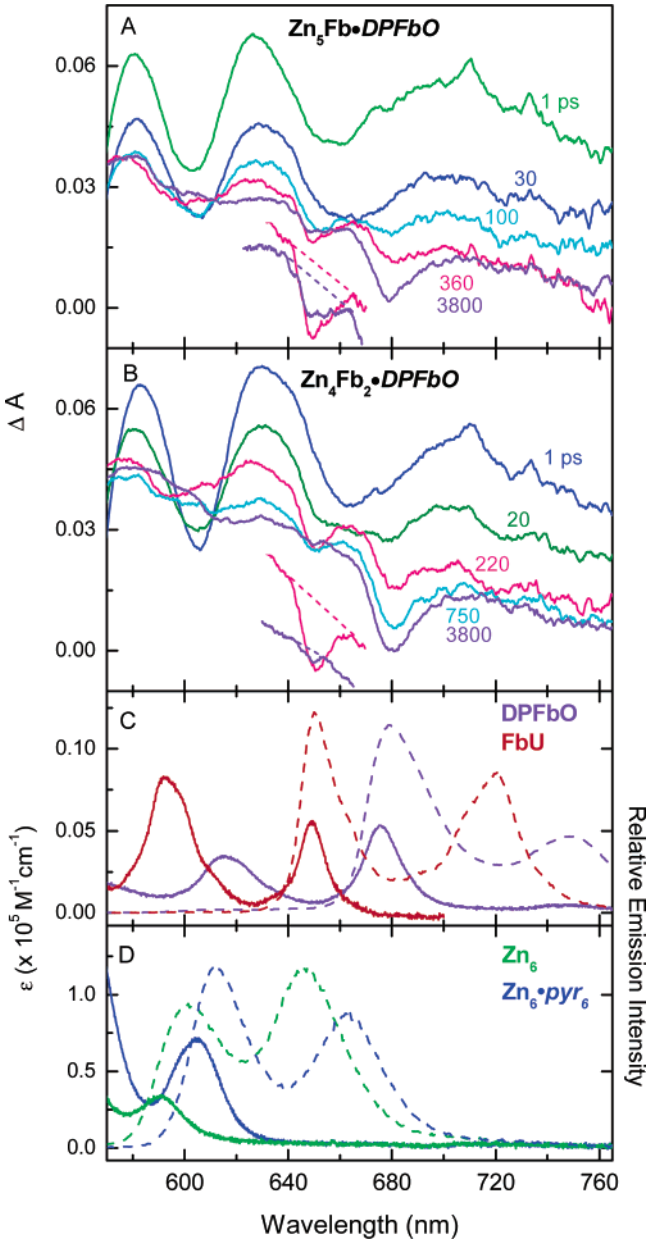

Figure 5. Transient-absorption spectra obtained using a 130 fs excitation flash at 540 nm for (A) Zn_5Fb·DPFbO and (B) Zn_4Fb_2·DPFbO. Panels C and D show absorption (solid lines) and fluorescence (dashed lines) spectra of DPFbO (violet), FbU (red), Zn_6 (green), and Zn_6·pyr_6 (blue).

Fb* in the host (Charts 2B and 3D). We expect a contribution from this same unit along with the other Fb porphyrin in Zn_4Fb_2·DPFbO, which is expected to have a lifetime of ~0.5 ns on the basis of the transient-absorption data. The fluorescence-decay profile for Zn_4Fb_2·DPFbO at 650 nm is well described by a time constant of 1.7 ns and also can be fit well with components of 8 ns (fixed) and 0.8 ± 0.3 ns. These values are utilized below in conjunction with the transient-absorption data to derive the rate constants and yields for energy transfer.

a. Transient-Absorption Studies on Zn_5Fb·DPFbO. Time-resolved absorption difference spectra for Zn_5Fb·DPFbO are shown in Figure 5A. Static absorption and fluorescence spectra of reference monomers and cyclic hexamers are shown in Figures 5C and 5D. The reference spectral profiles identify the contributions to the ground-state absorption bleaching and excited-state stimulated-emission features in the transient-state spectra.

The 1 ps spectrum is due primarily to Zn_U^*, with some contribution from the other components of the complex that absorb a fraction of the excitation light, including the bookend porphyrins Zn_C. By 30 ps, the population of Zn_C^* has grown appreciably due to $Zn_U^*Zn_C \rightarrow Zn_UZn_C^*$ energy transfer, as is indicated by the expected red shift in the features. By 100 ps, energy has arrived on the Fb porphyrin in the hexameric host, as is indicated by the formation of the combined Fb* Q(0,0) stimulated emission and bleaching at ~650 nm and the Q(0,1) stimulated emission at ~720 nm (compare with the red spectra in Figure 5C). Some Zn_C^* still remains, as is indicated by the dip at ~610 nm (compare with the blue spectra in Figure 5D), and is assigned to the Zn_C unit bounded by two, higher-energy Zn_U units (lower left of Chart 3D and porphyrin 5 in Chart 2B). Some energy may also be present on the DPFbO guest at 100 ps, as is demonstrated by the combined Q(0,0) bleaching and stimulated-emission feature at ~680 nm (compare with the violet spectra in Figure 5C). It is possible that some of this DPFbO* is produced directly upon excitation and is present but masked by the main features at earlier times. The spectrum continues to evolve, and at 360 ps the DPFbO* contribution has grown somewhat while those due to Zn_C^* and Fb* have diminished but remain substantial. By 3800 ps, the DPFbO* features have notably increased in amplitude, the ~610 nm feature due to Zn_C^* has essentially disappeared, and the dip at ~650 nm due to Fb* has diminished but is still present (see the expanded view in Figure 5A). The time evolution of the spectra is described well by three components with time constants of 3 ± 1 ps, 30 ± 10 ps, and 400 ± 100 ps (Supporting Information). As noted above for other arrays containing adjacent zinc porphyrins, the minor fast phase is assigned to excited-state annihilation in a small fraction of the arrays. The other two components reflect energy flow in the Zn_5Fb·DPFbO complex (Charts 2B and 3D), as is described below.

It is clear from the transient-absorption data that two members of the Zn_5Fb hexameric host are effective energy donors to the DPFbO guest, namely, the Fb porphyrin (porphyrin 1 in Chart 2B and top unit in Chart 3D) and its nonadjacent Zn_C (porphyrin 5 in Chart 2B and lower left of Chart 3D). After light absorption, the Fb and nonadjacent Zn_C units are fed by the other zinc porphyrins of the host with an effective time constant of 30 ps, derived from the transient-absorption kinetics. This phase is successfully modeled using rate constants for the individual processes obtained from the simpler arrays described above and in the companion paper.[1] Subsequently, the nonadjacent Zn_C^* and Fb* decay in parallel. We first consider the former process.

The nonadjacent Zn_C^* decays by three pathways (Chart 3D): (1) the internal routes active in the absence of energy transfer (fluorescence, internal conversion, intersystem crossing) with a combined rate constant $k_{Zn} = (2.1\ ns)^{-1}$, obtained from Zn_6·pyr_6 in the companion paper;[1] (2) energy transfer to the guest with rate constant $M_4 = (0.73\ ns)^{-1}$, determined from Zn_6·DPFbO; (3) superexchange-mediated energy transfer to the Fb porphyrin (L_3). The nonadjacent Zn_C^* lifetime in Zn_5Fb·DPFbO is then $\tau = (k_{Zn} + M_4 + L_3)^{-1}$, which we equate with the 400 ps component in the transient-absorption dynamics. Furthermore, we know that $\tau = (k_{Zn} + M_4)^{-1} = 540$ ps from the analogous decay of Zn_C^* in Zn_6·DPFbO, which lacks the energy transfer to a Fb porphyrin (Chart 3B). Hence, the relative lifetimes of the two arrays are consistent and afford an energy-transfer rate from the nonadjacent Zn_C to the Fb porphyrin in Zn_5Fb·DPFbO of $L_3 = (400\ ps)^{-1} - (540\ ps)^{-1} \approx (1.5\ ns)^{-1}$. Thus, the relative fractions of nonadjacent Zn_C^* decay due to different processes are as follows: internal deactivation, [(400 ps)/(2.1 ns)] = 0.19; energy transfer to the guest, [(400 ps)/(730 ps)] = 0.54; energy transfer to the Fb porphyrin (which is also a donor to the guest), [(400 ps)/(1.5 ns)] = 0.27. The fact that the latter value is appreciable indicates that energy transfer to the Fb porphyrin from the nonadjacent Zn_C^* plays a significant role in the overall excited-state dynamics in this array.

A fraction of the energy harvested by the hexamer is delivered to the Fb porphyrin in Zn_5Fb·DPFbO to produce Fb*, which decays as follows. The Fb* excited state has a lifetime of 8 ns determined above from the time-resolved fluorescence at 650 nm. In comparison to 13 ns for Fb porphyrin reference compounds, this lifetime gives a yield of $[1 - (8/13)] = 0.38$ and an effective rate constant of $M_8 + N_2 = [(8\ ns)^{-1} - (13\ ns)^{-1}] \approx (20\ ns)^{-1}$ for Fb* DPFbO → Fb DPFbO* energy transfer. This overall rate encompasses direct TS and Zn_C superexchange-mediated routes (Chart 3D). The superexchange-mediated pathway will be significantly slower than the direct TS pathway, for which $M_4 = (0.73\ ns)^{-1}$. The TS route from the Fb porphyrin to the guest (M_8) is calculated to have a Förster efficiency $\Phi_{TS} = 0.57$ and rate $k_{TS} = (9.7\ ns)^{-1}$ (Table 3).[31] The latter rate is somewhat greater than $M_8 + N_2 \approx (20\ ns)^{-1}$ but is in reasonably good accord.

The above analysis provides in-depth insights into the major routes of energy flow in Zn_5Fb·DPFbO, including the yields of energy transfer to the DPFbO guest from Fb* and the nonadjacent Zn_C^* (porphyrins 1 and 5 in Chart 2B). The overall quantum yield of energy transfer to the host will be $\Phi_{trans} = 0.54f_{Zn} + 0.38(f_{Fb} + 0.27f_{Zn})$. Here, f_{Zn} and f_{Fb} are the fractions of the excitation that reside on the Fb and nonadjacent Zn_C energy-donor units following excitation. (Note that $f_{Zn} + f_{Fb} \cong 1$, because energy migration within the hexamer to the two donors is essentially quantitative.) The term $(0.38 \times 0.27f_{Zn})$ derives from the nonadjacent energy transfer from Zn_C^* to the Fb unit (L_3; Chart 3D). When f_{Zn} is 0, 0.25, 0.5, 0.75, or 1, then Φ_{trans} is 0.38, 0.45, 0.51, 0.58, or 0.64, respectively. The yield is also obtained from simulations using the model in Chart 3D with the rate constants derived above. The simulations give $\Phi_{trans} = 0.53$ if the initial excitation is proportioned between the three Zn_U units of the hexamer or among all five zinc porphyrins, and $\Phi_{trans} = 0.51$ for equal excitation of all six porphyrins of the host.

The above results show that energy trapping by Zn_5Fb·DPFbO is somewhat smaller than that in Zn_6·DPFbO, which has a yield $\Phi_{trans} = 0.74$. Closer examination of the rate constants and kinetic models (Charts 3B and 3D) indicates that the overall trapping yield is not enhanced in Zn_5Fb·DPFbO relative to that in Zn_6·DPFbO because of the much slower rate of energy trapping from the Fb porphyrin (M_8) versus a Zn_C porphyrin (M_4). The analysis further indicates that this difference in rates derives from the longer distance for the former process compared to the latter, which enters into the Förster TS rate as R^{-6}. The longer distance to the donor completely eliminates the beneficial effect of the ~6-fold longer lifetime of the Fb porphyrin way station in Zn_5Fb·DPFbO. Examination of the structures indicates that a more favorable position for the Fb porphyrin in the hexamer would be at the position trans to its location in Zn_5Fb·DPFbO (Chart 3D). In this regard, for Zn_4Fb_2·DPFbO, one of the two Fb porphyrins does in fact reside at this position in the array (Charts 2A and 3C). This architectural feature alters the energy flow in Zn_4Fb_2·DPFbO versus that in Zn_5Fb·DPFbO, as will be described in the following section.

b. Transient-Absorption Studies on Zn_4Fb_2·DPFbO. Time-resolved absorption difference spectra for Zn_4Fb_2·DPFbO are shown in Figure 5B. Assignment of the spectra utilizes the reference spectra shown in Figures 5C and 5D and follows the logic described above for Zn_5Fb·DPFbO. The pathways for energy flow in this array are illustrated in Chart 3C.

The 1 ps spectrum is primarily associated with a mixture of Zn_U^* and Zn_C^*. The spectrum continues to evolve, including the growth of features due to Fb* (e.g., ~650 nm), which dominates the spectrum by 220 ps. At that time, some energy also resides on the DPFbO guest (~680 nm feature), a fraction of which may have been present and masked at earlier times. The spectra continue to evolve, and by 3800 ps the features due to DPFbO* have clearly increased in amplitude, accompanied by a substantial decrease in those due to the hexamer Fb*. The expanded views of this region in Figures 5A and 5B show that the Fb* feature at ~650 nm has decayed to ~85% of its maximal amplitude by 3800 ps for Zn_4Fb_2·DPFbO, compared to ~48% for Zn_5Fb·DPFbO. The analysis below shows that this latter difference is reflective of more facile energy flow to the guest in the former array.

The time evolution of the transient-absorption spectra for Zn_4Fb_2·DPFbO is well described by two components with time constants of 30 ± 10 ps and 510 ± 30 ps (Supporting Information). The 30 ps component is modeled well using the rate constants from the simpler arrays. This component is due to energy flow among the units of the hexamer to produce, in parallel, the Fb* excited states of the two Fb porphyrins, which are the lowest-energy sites in the Zn_4Fb_2 host (Charts 3C and 3G).

The 510 ps component is assigned to the lifetime of the Fb porphyrin that has the shortest center-to-center distance (14.2 versus 20.9 Å; Chart 2A) to the guest (bottom unit in Chart 3C and porphyrin 4 in Chart 2A). This Fb* lifetime is a combination of (1) internal deactivation with a rate constant of $(13\ \text{ns})^{-1}$ from reference compounds, (2) TS energy transfer (M_7) to the DPFbO guest with a calculated Förster rate constant $k_{TS} = (0.96\ \text{ns})^{-1}$ and efficiency $\Phi_{TS} = 0.93$ (Table 3), and (3) nonadjacent transfer via Zn_C (N_1), which will have a rate constant smaller than $M_4 = (730\ \text{ps})^{-1}$. Comparison of the measured lifetime of this Fb porphyrin with that in the absence of energy transfer gives a yield of $[1 - (0.51/13)] = 0.96$ and an effective rate constant $M_7 + N_1 = [(0.51\ \text{ns})^{-1} - (13\ \text{ns})^{-1}] = (0.53\ \text{ns})^{-1}$ for energy transfer from this host unit to the guest. The measured and calculated TS rate constants and yields for Fb*DPFbO → Fb DPFbO* for Zn_4Fb_2·DPFbO are in good accord and indicate that this donor (porphyrin 4 in Chart 2A) affords an efficient route for TS energy transfer to the guest due to the relatively short distance involved. However, the lifetime of the Fb porphyrin more distant from the guest (top in Chart 3C and porphyrin 1 in Chart 2A) is expected to have a yield of 0.38 and rate $M_8 + N_2 \approx (20\ \text{ns})^{-1}$ based on the studies of Zn_5Fb·DPFbO.

Thus, the overall yield of energy transfer to the guest in Zn_4Fb_2·DPFbO will be $\Phi_{trans} = 0.96f_{Fb1} + 0.38f_{Fb2}$. Due to the symmetry of the array, $f_{Fb1} = f_{Fb2} = 0.5$, assuming essentially quantitative energy transfer from the zinc porphyrins of the host to the Fb units, as is expected from studies on the simpler arrays. Thus, the overall energy-transfer yield will be 0.67. The simulations using the rate constants and kinetic model (Chart 3C) bear this out and give 0.68 whether the initial excitation resides on the two Zn_C porphyrins or equally among all six porphyrins in the hexamer. This yield is larger than that of 0.53 for Zn_5Fb·DPFbO. Thus, utilization of the energy-donor Fb porphyrin with the shorter, more efficient energy-transfer route to the guest has a beneficial impact on the light-harvesting efficiency.

IV. Conclusions

The three wheel-and-spoke complexes Zn_6·DPFbO, Zn_5Fb·DPFbO, and Zn_4Fb_2·DPFbO have numerous routes for energy flow within the hexameric hosts and to the porphyrin guests. The harvested excitation energy flows between adjacent and nonadjacent members of a hexamer and is delivered to the lowest-energy site(s) in the host with an effective rate constant of $(30-40\ \text{ps})^{-1}$ and with essentially quantitative yield (≥98%). The subsequent dynamics of energy transfer to the central guest porphyrin dictate the overall rate and yield of energy trapping.

The host-to-guest energy-transfer step for Zn_6·DPFbO (M_4) occurs from the bookend Zn_C porphyrins of the host with a yield of ~75%. Excitation energy moves from the host to the guest in Zn_5Fb·DPFbO in parallel using the Fb porphyrin [$M_8 \approx (20\ \text{ns})^{-1}$] and the nonadjacent Zn_C porphyrin [$M_4 \approx (0.7\ \text{ns})^{-1}$], with a combined yield of ~50%. Energy flows to the guest in Zn_4Fb_2·DPFbO via the same Fb porphyrin site as in Zn_5Fb·DPFbO (M_8) and from the second Fb porphyrin [$M_7 \approx (0.5\ \text{ns})^{-1}$], with an overall yield of ~70%. The rates and yields in all three arrays are comparable to those obtained from Förster calculations, and the differences derive primarily from the distances involved between the energy donors in the hexamer and the guest acceptor.

The rate constants derived herein indicate that minor changes in the pigment locations in the Zn_5Fb·DPFbO and Zn_4Fb_2·DPFbO arrays will afford substantially higher energy-transfer yields. For example, a swap in position of one of the Zn_U and the Fb porphyrin in Zn_5Fb·DPFbO that places the Fb porphyrin at ~14 Å rather than ~20 Å from the guest (i.e., a Zn_5Fb·DPFbO array wherein the Fb porphyrin is at position 4, see Chart 2B) should boost the overall energy trapping efficiency from ~50% to ~85%. A similar swap in Zn_4Fb_2·DPFbO that places both Fb porphyrins ~14 Å from the guest (i.e., a Zn_4Fb_2·DPFbO array wherein the Fb porphyrins are at positions 4 and 6, see Chart 2A) should increase the efficiency from ~70% to ~90%.

Collectively, the studies reported herein elucidate the pathways, mechanisms, rates, and yields for energy transfer in the self-assembled host−guest complexes. The results provide valuable information for the design of next-generation light-harvesting systems for use in artificial solar-energy conversion systems. Key points from the studies reported in this and the companion paper are as follows: (1) Electronic coupling afforded by a pyridyl linker coordinated to a zinc porphyrin is too weak to support TB energy transfer. Accordingly, all routes to the central guest are essentially TS in character, whether via a Fb porphyrin unit or a linker-coordinated zinc porphyrin in the host. (2) The host site closest to the guest provides the most effective pathway for TS energy flow and should be occupied by the lowest-energy chromophore in the host for optimum excitation trapping. (3) All of the TS energy-transfer processes will potentially increase in rate upon use of chlorins, bacteriochlorins, or phthalocyanine species, all of which have increased oscillator strength for the long-wavelength transition.

Acknowledgment. This research was supported by grants from the Division of Chemical Sciences, Office of Basic Energy Sciences, Office of Energy Research, U. S. Department of Energy (J.S.L., D.F.B., and D.H.).

Note Added after ASAP Publication. The authorship of the paper has been revised from the version published September 13, 2006; the revised version was published September 20, 2006.

Supporting Information Available: Titration data for the formation of host−guest complexes and time-resolved absorption and kinetic data. This material is available free of charge via the Internet at http://pubs.acs.org.

References and Notes

(1) Song, H.; Kirmaier, C.; Schwartz, J. K.; Hindin, E.; Yu, L.; Bocian, D. F.; Lindsey, J. S.; Holten, D. *J. Phys. Chem. B* **2006**, *110*, 19121−19130.

(2) Imahori, H. *J. Phys. Chem. B* **2004**, *108*, 6130−6143.

(3) Choi, M.-S.; Yamazaki, T.; Yamazaki, I.; Aida, T. *Angew. Chem., Int. Ed.* **2004**, *43*, 150−158.

(4) Sugiura, K.-I. *Top. Curr. Chem.* **2003**, *228*, 65−85.

(5) Kobuke, Y.; Ogawa, K. *Bull. Chem. Soc. Jpn.* **2003**, *76*, 689−708.

(6) Harvey, P. D. In *The Porphyrin Handbook*; Kadish, K. M., Smith, K. M., Guilard, R., Eds.; Academic Press: San Diego, CA, 2003; Vol. 18, pp 63−250.

(7) (a) Kim, D.; Osuka, A. *J. Phys. Chem. A* **2003**, *107*, 8791−8816. (b) Aratani, N.; Osuka, A. *Macromol. Rapid Commun.* **2001**, *22*, 725−740.

(8) (a) Gust, D.; Moore, T. A.; Moore, A. L. *Acc. Chem. Res.* **2001**, *34*, 40−48. (b) Gust, D.; Moore, T. A.; Moore, A. L. *Acc. Chem. Res.* **1993**, *26*, 198−205. (c) Gust, D.; Moore, T. A. *Top. Curr. Chem.* **1991**, *159*, 103−151.

(9) Burrell, A. K.; Officer, D. L.; Plieger, P. G.; Reid, D. C. W. *Chem. Rev.* **2001**, *101*, 2751−2796.

(10) Hori, T.; Aratani, N.; Takagi, A.; Matsumoto, T.; Kawai, T.; Yoon, M.-C.; Yoon, Z. S.; Cho, S.; Kim, D.; Osuka, A. *Chem.—Eur. J.* **2006**, *12*, 1319−1327.

(11) Hwang, I.-W.; Yoon, Z. S.; Kim, J.; Kamada, T.; Ahn, T. K.; Aratani, N.; Osuka, A.; Kim, D. *J. Photochem. Photobiol., A* **2006**, *178*, 130−139.

(12) Hajjaj, F.; Yoon, Z. S.; Yoon, M.-C.; Park, J.; Satake, A.; Kim, D.; Kobuke, Y. *J. Am. Chem. Soc.* **2006**, *128*, 4612−4623.

(13) Kuramochi, Y.; Satake, A.; Kobuke, Y. *J. Am. Chem. Soc.* **2004**, *126*, 8668−8669.

(14) Nakamura, Y.; Hwang, I.-W.; Aratani, N.; Ahn, T. K.; Ko, D. M.; Takagi, A.; Kawai, T.; Matsumoto, T.; Kim, D.; Osuka, A. *J. Am. Chem. Soc.* **2005**, *127*, 236−246.

(15) Hwang, I.-W.; Park, M.; Ahn, T. K.; Yoon, Z. S.; Ko, D. M.; Kim, D.; Ito, F.; Ishibashi, Y.; Khan, S. R.; Nagasawa, Y.; Miyasaka, H.; Ikeda, C.; Takahashi, R.; Ogawa, K.; Satake, A.; Kobuke, Y. *Chem.—Eur. J.* **2005**, *11*, 3753−3761.

(16) Kato, A.; Sugiura, K.-I.; Miyasaka, H.; Tanaka, H.; Kawai, T.; Sugimoto, M.; Yamashita, M. *Chem. Lett.* **2004**, *33*, 578−579.

(17) Satake, A.; Kobuke, Y. *Tetrahedron* **2005**, *61*, 13−41.

(18) Balaban, T. S.; Tamiaki, H.; Holzwarth, A. R. *Top. Curr. Chem.* **2005**, *258*, 1−38.

(19) Drain, C. M.; Bazzan, G.; Milic, T.; Vinodu, M.; Goeltz, J. C. *Isr. J. Chem.* **2005**, *45*, 255−269.

(20) Alessio, E.; Iengo, E.; Marzilli, L. G. *Supramol. Chem.* **2002**, *14*, 103−120.

(21) Chambron, J.-C.; Heitz, V.; Sauvage, J.-P. In *The Porphyrin Handbook*; Kadish, K. M., Smith, K. M., Guilard, R., Eds.; Academic Press: San Diego, CA, 2000; Vol. 6, pp 1−42.

(22) Imamura, T.; Fukushima, K. *Coord. Chem. Rev.* **2000**, *198*, 133−156.

(23) Wojaczynski, J.; Latos-Grazynski, L. *Coord. Chem. Rev.* **2000**, *204*, 113−171.

(24) (a) Mongin, O.; Schuwey, A.; Vallot, M.-A.; Gossauer, A. *Tetrahedron Lett.* **1999**, *40*, 8347−8350. (b) Rucareanu, S.; Mongin, O.; Schuwey, A.; Hoyler, N.; Gossauer, A.; Amrein, W.; Hediger, H.-U. *J. Org. Chem.* **2001**, *66*, 4973−4988. (c) Rucareanu, S.; Schuwey, A.; Gossauer, A. *J. Am. Chem. Soc.* **2006**, *128*, 3396−3413.

(25) Li, J.; Ambroise, A.; Yang, S. I.; Diers, J. R.; Seth, J.; Wack, C. R.; Bocian, D. F.; Holten, D.; Lindsey, J. S. *J. Am. Chem. Soc.* **1999**, *121*, 8927−8940.

(26) Yu, L.; Lindsey, J. S. *J. Org. Chem.* **2001**, *66*, 7402−7419.

(27) Hsiao, J.-S.; Krueger, B. P.; Wagner, R. W.; Johnson, T. E.; Delaney, J. K.; Mauzerall, D. C.; Fleming, G. R.; Lindsey, J. S.; Bocian, D. F.; Donohoe, R. J. *J. Am. Chem. Soc.* **1996**, *118*, 11181−11193.

(28) Ambroise, A.; Li, J.; Yu, L.; Lindsey, J. S. *Org. Lett.* **2000**, *2*, 2563−2566.

(29) Hindin, E.; Forties, R. A.; Loewe, R. S.; Ambroise, A.; Kirmaier, C.; Bocian, D. F.; Lindsey, J. S.; Holten, D.; Knox, R. S. *J. Phys. Chem. B* **2004**, *108*, 12821−12832.

(30) del Rosario Benites, M.; Johnson, T. E.; Weghorn, S.; Yu, L.; Rao, P. D.; Diers, J. R.; Yang, S. I.; Kirmaier, C.; Bocian, D. F.; Holten, D.; Lindsey, J. S. *J. Mater. Chem.* **2002**, *12*, 65−80.

(31) In the Förster calculations (Table 3), a value of $\kappa^2 = 0.25$ has been used. This value is appropriate for energy transfer from a bookend porphyrin to the guest porphyrin assuming (1) free rotation of the guest relative to the host during the lifetime of the donor excited state (dynamically averaged limit) and (2) the transition-dipole direction in the DPFbO guest oxaporphyrin lies along the N−O axis. Förster energy transfer from a Fb porphyrin donor in the host to the DPFbO oxaporphyrin may have a larger κ^2 value; however, a value of $\kappa^2 = 0.25$ has also been used for this process to maintain consistency.

(32) Dixon, J. M.; Taniguchi, M.; Lindsey, J. S. *Photochem. Photobiol.* **2005**, *81*, 212−213.